Available online at www.sciencedirect.com

ScienceDirect

IFAC PapersOnline CONFERENCE PAPER ARCHIVE

IFAC PapersOnLine 55-9 (2022) 36–41

Phasor measurement unit based local fault detection in distribution systems

Márton Greber * **Attila Fodor** * **Attila Magyar** *

* *Department of Electrical Engineering and Information Systems, Faculty of Information Technology, University of Pannonia, Egyetem u. 10., Veszprém, H-8200, Hungary(e-mail: greber.marton, fodor.attila, magyar.attila@virt.uni-pannon.hu).*

Abstract: Distribution systems with advanced metering infrastructure offer many opportunities for fault detection. A novel approach is presented in this paper for local fault diagnosis in neighbour area networks by utilizing data concentrators. A lightweight local diagnostic function is presented based on first engineering principles. It is shown that from four phasor measurement unit data, a fault can be detected between buses and fault parameters can be evaluated. The diagnosis of a neighbour area network is accomplished as a sequential application of the local method. Edge cases and limitations of the method are explored. The applicability of the method is demonstrated on a real world case study. By introducing threshold values for the fault parameters, the results fulfill the engineering expectations.

Keywords: Smart grids; Computational methods for FDI; Modeling and simulation of power systems; Fault detection and diagnosis; Complex system management

NOMENCLATURE

f_{Diag}	Diagnostic function
I_f	Fault current
I_k	Current at customer k
$n,\ Bus_n$	Node indexing
$n, n+1$	Edge delimited by buses n and $n+1$
U_k	Bus voltage at node k
$\boldsymbol{x}$	Vector of diagnostic input parameters
$\boldsymbol{x}\|_{shift=k}$	Input parameters at sift position k
$\boldsymbol{y}$	Vector of fault parameters
Z_f	Fault distance representing impedance

1. INTRODUCTION

The power distribution system is exposed to various kind of faults, which can originate from different sources like weather, environmental objects or malicious human activity. If a tree falls on the distribution line or a pole is damaged, the live wire is connected to ground. Since cables are insulated and most of the faulty objects have low conductivity these are called high impedance faults (HIF). Moreover, faulty connections can also be caused by human activities, motivated by power theft. These faults produce non-technical losses (NTL). HIF is likely to be accompanied with arcs and can contribute to harmonic distortion. Whereas NTL can lead to the malfunction of the grounding system. Since these are not short-circuit like faults, protective gear is not necessarily triggered. This category of quasi-steady state faults is called persistent faults (PF), since faulty operation can go unnoticed for longer periods of time.

Long existing detection methods in medium-voltage networks are based on the fact that PFs can cause high frequency distortions, which can be analyzed. (Aucoin and Russell (1982)) On the other hand if these are not present, special test signals can be injected from the distribution feeder into the network and the response can be further analyzed. (Jota and Jota (1998)) This problem is related to classification where approximate solutions can be found using soft computing techniques. The bottleneck of this approach is that the injection and high-resolution data acquisition (DAQ) is done at the distribution feeder point, as a result there is not enough data for isolation.

In order to tackle this problem, networks with advanced metering infrastructure (AMI) enable better spatial resolution for detection. In AMI networks, consumption is monitored and the flow of information is enabled through communication channels. AMI is continuously upgraded with respect to both hardware and software. Since it has a reliable technological foundation it is well suited for diagnostic purposes. According to the type of the measurement device, two arts are distinguished: smart meters (SM) and phasor measurement units (PMU). Smart meters are the commercial grade device, which are capable for measuring root-mean squared (RMS) voltage, current, active and reactive power. On the other hand phasor measurement units are capable of measuring complex current and voltage values. (Penshanwar et al. (2015))

The gathered data is then sent to a data center, where analysis can be accomplished. Having all the network parameters and topology data at hand, the state of the network can be simulated. Using the consumption data at the loads, the bus voltages can be calculated. Comparing the simulated and the measured bus voltages, gives an indicator for the presence of faults. (Bula et al. (2016)) The unknown parameters for a fault are the distance form the adjacent buses and the fault current. In case there is a difference between simulated and measured quantities, the

10.1016/j.ifacol.2022.07.007

simulated network needs to be extended with faults in such a way that it minimizes this voltage difference. In case of transmission lines it was shown, that by knowing the fault current, the fault can be located on a line segment just by using one terminal measurement. (Takagi et al. (1982)) On the other hand if the fault location is known, the fault current can be estimated using SM data just by using RMS values. (Kodaira and Han (2018)) However in case of real world networks, the search space for such optimization problem is enormous. More diagnostic calculations need to be done on the utility server side, which means that data traffic will be increased. However sending additional fault flags with each smart meter reading would increase the data traffic. As a study showed, 2 million homes can generate 22 GB of data per day (Rusitschka et al. (2010)), therefore search space reduction techniques are sought. The aim of this work is to present a local, model based detection method for determining the fault location and current, by utilizing PMU measurement data.

2. DIAGNOSIS ON DATA CONCENTRATOR LEVEL

As mentioned before, AMI consists of the metering equipment and the associated communication channels (see figure 1). A neighbourhood of consumers equipped with smart meter is connected to a neighbour area network (NAN). Data from this region is collected by a data concentrator, which is connected to the wide area network(WAN). (Ornelas et al. (2016)) From this point data arrives at the providers data center, where logging and monitoring happens with a sampling time of 15 minutes. Fault detection can be applied locally, if the evaluation method involves more than one smart meter reading. Moreover, local network parameters and topology information needs to be available for model based diagnosis. Taking into consideration that data concentrators offer more computational resources than smart meters (e.g.: TI's AM335x is equipped with Cortex - A8 processor (Prakash (2018))) they are suitable for this task. This means that a NAN can be evaluated for faults on the data concentrator level.

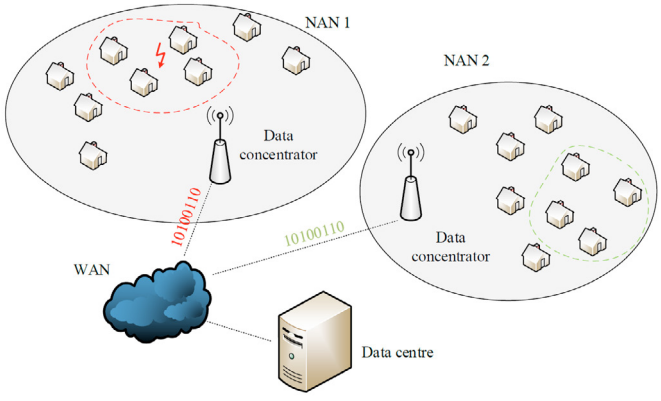

Fig. 1. Diagnosis in advanced metering infrastructure: if a group of customers is affected by a fault, after detection by the data concentrator, the utility is notified (red area); else confirmation about proper network operation is sent (green area)

Existing time domain local fault diagnosis methods are executed on a so called 'T' structure, taking measurements from two adjacent loads, and diagnosing the edge connecting the two for fault. (Le et al. (2016), Chakraborty and Das (2019)) However for quasi-steady state diagnosis this structure alone is underdetermined. One nodal equation in the center of the 'T' according to Kirchhoff's current law(KCL) results in three unknowns: the distance, the fault current and the nodal voltage at the fault point. The proposed local evaluation method takes four neighbouring, metered nodes in a series configuration and evaluates this segment. Smart power distribution systems are mainly equipped with SMs on residential consumers, PMUs are common in transmission systems. In order to emphasize the diagnostic method over the underlying numerical equations, the method is presented using PMU data. Nevertheless the method is still applicable with either metering device. With PMUs one obtains a set of linear equations, on the other hand with SMs these are nonlinear equations. (Greber et al. (2020)) The NAN is diagnosed in small groups of four nodes. The method is based on current and voltage meter readings at the customer connection points, and has algebraic solution(or iterative in the case of SMs), no online optimization is necessary. Keeping the calculation method lightweight is key, in order to be able to diagnose the given NAN for every 15 minutes period. In case a fault happens, the periodical, consumption data package is extended with the fault parameters, therefore the increase in communication overhead is minimal.

3. FAULT DETECTION METHOD

The local evaluation methodology is explained using just single line representation, the structure of the detection segment is shown in figure 2. A lumped parameter three wire network is considered with solid grounding therefore the neutral is eliminated. Residential customers and faults are modeled as ideal current sources. The distribution lines consists of RL branches, where capacitance and mutual coupling is neglected. Throughout the work, impedance is used interchangeably with length, because cable parameters are specified per unit length. Since PMU data is used, all the electrical quantities are complex numbers. The initial thought process begins by taking two consumers connected to nodes n_2 and n_3, the impedance between these nodes is Z_2. Assume, that there is a fault between these nodes at a distance represented by Z_f , where $0 < Z_f < Z_2$. Then Z_2 can be divided into two parts: Z_f and $Z_2 - Z_f$. The fault current is represented by I_f . This construct allows us to insert one fault at an arbitrary position between n_2 and n_3. This results in three unknown variables in the structure: Z_f , I_f and U_{n_f} . In order to solve this problem let us use Kirchhoff's current law (KCL) on node n_f :

$$I_{Z_f} + I_{Z_2 - Z_f} - I_f = 0. \tag{1}$$

The distribution line currents can be expressed in terms of bus voltages:

$$\frac{U_{n_2} - U_{n_f}}{Z_f} + \frac{U_{n_3} - U_{n_f}}{Z_2 - Z_f} - I_f = 0. \tag{2}$$

It is easy to see, that equation (2) is underdetermined, i.e. it cannot be solved exactly, therefore two more equations are needed. The same procedure as shown in equations (1) and (2) should be done for nodes n_2 and n_3. However in order to be able to formulate these equations the nodes

next to n_2 and n_3 should be brought into the evaluation structure. This is the reason why the fault diagnosis structure consists of four metered PMU nodes.

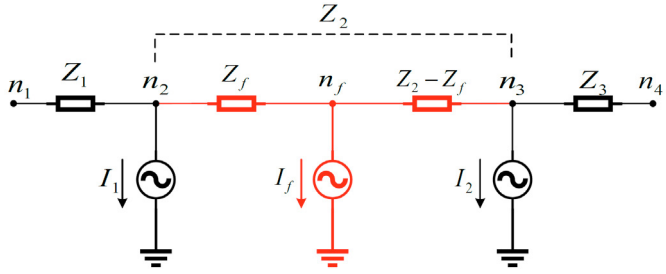

Fig. 2. Local evaluation structure: $n_1 \dots n_4$ are metered nodes, whereas n_f represents the inserted hypothetical fault node with a fault current of I_f. The fault location is defined as the impedance from n_2 as Z_f.

By arranging the 3 KCL equations together, the following equation system is obtained:

$$\begin{cases} \dfrac{U_{n_1}-U_{n_2}}{Z_1}+\dfrac{U_{n_f}-U_{n_2}}{Z_f}-I_1=0 \ : \ \text{node } n_2 \\ \dfrac{U_{n_2}-U_{n_f}}{Z_f}+\dfrac{U_{n_3}-U_{n_f}}{Z_2-Z_f}-I_f=0 \ : \ \text{node } n_f \\ \dfrac{U_{n_f}-U_{n_3}}{Z_2-Z_f}+\dfrac{U_{n_4}-U_{n_3}}{Z_3}-I_2=0 \ : \ \text{node } n_3. \end{cases} \tag{3}$$

The bus voltage at n_f is of no use with regards to the detection process, therefore it can be eliminated. The system can be rearranged in terms of the fault parameters: I_f and Z_f:

$$\begin{cases} I_f = \dfrac{U_{n_4}Z_1 - U_{n_3}Z_1 + (U_{n_1} - U_{n_2} - (I_1+I_2)Z_1)Z_3}{Z_1 Z_3} \\ Z_f = \dfrac{Z_1(-U_{n_4}Z_2 - U_{n_2}Z_3 + I_{n_2}Z_2Z_3 + U_{n_3}(Z_2+Z_3))}{U_{n_3}Z_1 - U_{n_4}Z_1 + (U_{n_2} - U_{n_1} + (I_1+I_2)Z_1)Z_3}. \end{cases} \tag{4}$$

The above equations represent the solution for the evaluation of the diagnostic model. For further references this calculation is described as a function f_{Diag} (diagnostic function), which relates the PMU voltage and current measurements and the impedance parameters ($\boldsymbol{x}$) to the fault parameters ($\boldsymbol{y}$):

$$\left.\begin{aligned} \boldsymbol{x}^T &= [U_{n_1}\ U_{n_2}\ U_{n_3}\ U_{n_4}\ I_1\ I_2\ Z_1\ Z_2\ Z_3] \\ \boldsymbol{y}^T &= [I_f\ Z_f] \end{aligned}\right\}$$
$$\boldsymbol{y} = f_{Diag}(\boldsymbol{x}),\ f_{Diag} : \mathbb{C}^9 \to \mathbb{C}^2 \tag{5}$$

3.1 NAN segment evaluation

A group of 4 consumers can be diagnosed with f_{Diag}. It is presented how the repetitive application of this method by the data concentrator can evaluate a whole NAN. The dominating topological structure in low-voltage distribution networks is a long series configuration, also called street. Therefore the NAN evaluation is presented on a series example structure, depicted in figure 3. For the sake of the explanation, just a single phase, one-line representation is considered. There are 8 customers connected to $Bus_1 \dots Bus_8$ appropriately, a hidden fault is inserted between buses Bus_4 and Bus_5.

At first, starting at the left side of the structure, the diagnostic function is evaluated by the data concentrator for buses $1 \dots 4$. By evaluating f_{Diag} there are two possible outcomes which can occur:

- if the fault current (y_1) is equal to zero, the segment is validated. In this case we don't care about the fault impedance (y_2) result,
- if the fault current is not zero, there is leak in the structure, the segment is marked as faulty.

Next, the diagnostic function is moved by one bus to the right in order to evaluate $Bus_2 \dots Bus_5$. This operation is referred as the shifting of f_{Diag}. The amount of buses by which it is shifted, is referred to the first position and it is noted by the shift variable. The notation $x|_{shift=1}$ means that the parameter values regarding $Bus_2 \dots Bus_5$ are substituted into the diagnostic function arguments; one example is: $U_{n_1} \leftarrow U_{Bus_2}$ in this case.

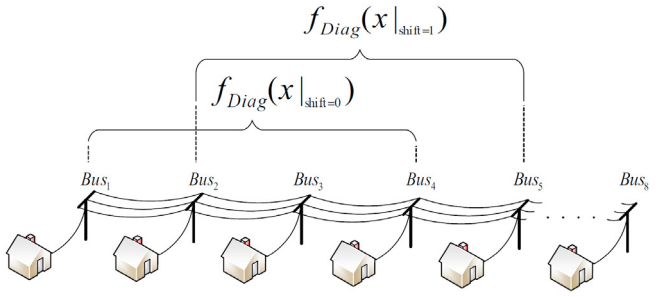

Fig. 3. The process of shifting the diagnostic function: at first the measurements regarding $Bus_1 \dots Bus_4$ are sent to the data concentrator and substituted into f_{Diag}. Next the perspective is shifted to the right by one unit($shift = 1$), and the section governed by $Bus_2 \dots Bus_5$ is evaluated etc.

The section of $Bus_2 \dots Bus_5$ is evaluated and labeled, either as validated or faulty like mentioned before. Then it is shifted again by one, meaning that the section of $Bus_3 \dots Bus_6$ is next up, this process is repeated until the end of the series structure. The results of the shifting process are shown in Table 1., where '✓' means validated and '✕' represents faulty.

Table 1. Results of the diagnostic function shifting

Shift value \ Bus index	1	2	3	4	5	6	7	8
0	✓	✓	✓	✓				
1		✕	✕	✕	✕			
2			✕	✕	✕	✕		
3				✕	✕	✕	✕	
4					✓	✓	✓	✓

At the initial position, the diagnostic function returns zero fault current, it is marked as validated. At $shift = 1$ we get non-zero fault current, because the hidden faulty branch between buses 4 and 5 is in the actual function evaluation range. However this fault current is just an indicator that in order for KCL to be true there must be some kind of compensation. The same holds for shift values 2 and 3, at position 4 the segment is valid again. f_{Diag} calculates the fault parameters between its actual n_2 and n_3 (at the middle of the 4 node structure). We need to find out the true fault, out of shifts 1, 2 and 3, in order to get correct

fault parameter values. To overcome this problem, more rules need to be introduced: if a set of nodes is validated through some arbitrary shift position, it is said that those are validated. The edges between those nodes are also truly valid. The truly faulty edges are obtained by subtracting all the validated edges from the set of faulty edges, where difference is considered as a set operation. Using the table above we can construct the set of truly validated and faulty edges. On a side note it should be mentioned that edges are defined through their endpoints, therefore they are described as number pairs. The intermediate result sets are the following:

$$\begin{aligned} \text{Validated} &= \{\{1,2\},\{2,3\},\{3,4\}\{5,6\},\{6,7\},\{7,8\}\} \\ \text{Faulty} &= \{\{2,3\},\{3,4\},\{4,5\},\{5,6\},\{6,7\}\} \\ \text{True faults} &= \text{Faulty} \setminus \text{Validated} = \{\{4,5\}\}. \end{aligned} \tag{6}$$

By using the fault parameters calculated at $shift = 2$, where buses 4 and 5 are in the middle, the correct fault parameters are obtained.

3.2 Limitations

Since the diagnostic function covers four nodes at a time, there are spatial limitations regarding the method. The first limitation is that fault parameters can't be calculated in the first and last edge in a series sequence. The reasoning is explained on the starting edge case, depicted on figure 4. In the best case if the section from Bus_2 to Bus_5 contains no faults we can isolate the fault in the first edge. By evaluating $f_{Diag}(x|_{shift=0})$ we get non-zero fault current, since there is deficit. Shifting the function by one results in no fault current in case of: $f_{Diag}(x|_{shift=1})$. It can be concluded that the first edge was the faulty one, however the fault parameters can't be determined. The same holds for the last edge on the line.

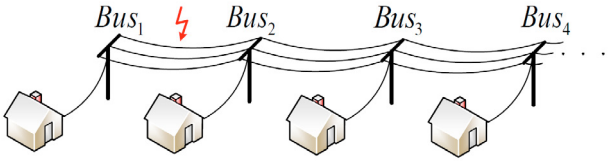

Fig. 4. Endpoint limitation : fault is present in the first edge. If $shift = 1$ is validated we can isolate the first edge, however no fault parameters can be calculated.

On the other hand if there are two or more faulty edges after each other, the fault parameters can't be calculated (see figure 5.). In this case the fault is interlocked. Approaching such a segment from left to right, the evaluation returns faulty if the diagnostic function reaches Bus_{i+2}. The faulty property holds until the left most node in the function is Bus_{i+3}. In this case the faulty edges can only be labeled as faulty without any further information about the fault parameters. In general it can be formulated the fault parameters can be calculated for edge $\{Bus_i, Bus_{i+1}\}$ if and only if the edges $\{Bus_{i-1},\ Bus_i\}$ and $\{Bus_{i+1}, Bus_{i+2}\}$ exist and are validated edges. The minimal distance between faulty locations of at least three edges or four buses is necessary for successful isolation. These two statements are the consequence of the length of f_{Diag}, the endpoint and the interlocked effects.

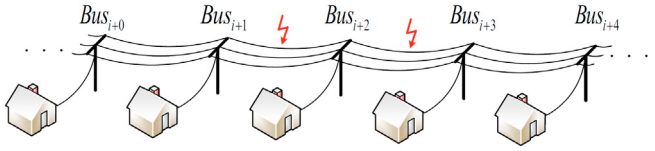

Fig. 5. Interlocked limitation: in case of consequent faults at non-endpoints, detection is only possible and the fault parameters can't be determined.

4. CASE STUDY

The real life applicability of the proposed methodology is evaluated through a simple case study. Typical low-voltage residential connections are depicted in figures 3, 4, 5. Consumers connect to the distribution lines through service cables. However this was neglected in the modeling section since these are of short length. Because the consumed current at a given point is much less than the current flowing in the distribution line and considering the short length of the service cable, voltage drop is negligible. Aside from presenting the method in operation, the goal of the case study has been to elaborate on this modeling assumption. How much error it incorporates into the detection and whether it can be handled in some way.

A real world low-voltage transformer area is used for the case study (see figure 6). The detailed operation of the network is recreated from the real world parameters. Then phasor data is gathered at consumer locations. These measurements are then fed to the data concentrator algorithm. Using the elaborated diagnostic function the network is evaluated for fault. This way the measurement data and network parameters represent the reality, and the diagnostic method, with all it's simplifications can be evaluated.

Fig. 6. Low-voltage test case topology. The red dashed neighbourhood denotes a series sequence of customers, which has been evaluated in case 2, through the shifting process of f_{Diag}

For better oversight examples are only explained for phase B, which is depicted by blue components on the topology. Let us first assume that on the top street there is no fault. The diagnostic function is evaluated for customers denoted by numbers $12, 8, 5$ and 2. The input parameters are shown in Tables 2 and 3.

Table 2. PMU measurement data for case 1.

Bus	Voltage$[V]$	Current$[A]$
12	$229.87\angle 120^o$	$0.731\angle 120^o$
8	$229.896\angle 120$	$0.422\angle 122.2^o$
5	$229.914\angle 120$	$1.294\angle 119.8^o$
2	$229.977\angle 120$	$0.645\angle 120^o$

Table 3. Impedance data for case 1.

Edge	Impedance$[m\Omega]$
$\{12;8\}$	$33.6 + 7.7i$
$\{8;5\}$	$22.1 + 5.0i$
$\{5;2\}$	$22.7 + 5.2i$

By evaluating f_{Diag}, a fault current of 0 is expected, since a fault free section is assumed. If service cable data is available, incorporating it in the calculations represents higher model fidelity. The residual current in this case is:

$$I_f^{'} = 0.0070016\angle -29.2871^o, \tag{7}$$

which is two orders of magnitude lower than the smallest registered consumption. However in most cases data about service cable connection is not available, therefore it is assumed to be zero. In this case a higher fault current is obtained

$$I_f^{''} = 0.29521\angle 117.3706^o. \tag{8}$$

This is only the effect of reduced model fidelity and numerical errors, however section $\{12, 8, 5, 2\}$ is still fault free. In order to avid such false positives a threshold value is introduced based on empirical experiments. If the fault current is less than all the PMU current values - regarding a given series section -, then it is a false positive, it should be neglected. Since $I_f^{''}$ is smaller in absolute value than all the currents in table 2., it can be concluded that this section is fault free.

Table 4. PMU measurement data for case 2.

Bus	Voltage$[V]$	Current$[A]$
46	$229.4234\angle 119.9779$	$0.936\angle 121.5^o$
43	$229.4248\angle 119.978$	$0.467\angle 111.19^o$
40	$229.4567\angle 119.9795$	$0.690\angle 114.69^o$
37	$229.4795\angle 119.9805$	$0.484\angle 117.06^o$
35	$229.5103\angle 119.9819$	$0.115\angle 126.42^o$
33	$229.5446\angle 119.9835$	$0.531\angle 110.3^o$
30	$229.5832\angle 119.9851$	$1.13\angle 110.86^o$
27	$229.6787\angle 119.9885$	$1.147\angle 113.3798^o$
15	$229.7887\angle 119.9922$	$0.355\angle 128.58^o$

As the second case, let us now observe the bottom part of the network, where a series segment staring with customer 46 and ending with 15 is highlighted. The fault currents depicted in figure 7 are obtained by shifting the diagnostic function through this part of the network. At first sight it would mean, that according to equation 6, the elements in-between shift positions $1 \ldots 5$ are interlocked. However, the fault threshold can be drawn based on the PMU data(see table 4). This will sort out positions 1 and 5 as false positives, the rest is done according the logic shown previously in table 1. Finally the fault parameters for $shift = 3$ can be extracted, a fault with a current magnitude of $0.315[A]$ was found. The network is build from cable type '4x95 Al', the positive sequence impedance is $0.311 + 0.071i[\Omega/km]$. By calculating the difference between diagnosed and actual fault impedance and translating it to distance, the difference is $1.1[m]$.

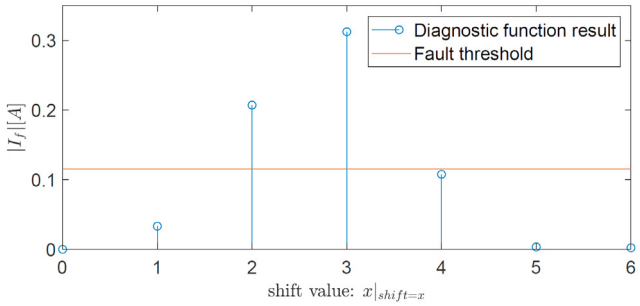

Fig. 7. Shift results of the diagnostic function for case 2 : the fault current magnitudes plotted against the shift values. $shift = 1$ and $shift = 5$ are sorted out since these are below the threshold value.

5. CONCLUSION

In this paper an approach has been presented for enabling local fault diagnosis on data concentrator level. The sources of measurement data has been chosen to be phasor measurement units. These allow to work with complex quantities, therefore offer higher model fidelity. A lightweight quasi-steady state local diagnostic function is derived based on KCL. It allows the evaluation of four consequent series nodes, by determining fault distance and fault current. On the other hand there are some limitations regarding different fault scenarios. These options have been explored and presented. Since the method implements algebraic equations it is computationally light, therefore it can be implemented on the data concentrator level. This offers the benefit of reducing additional communication overhead with regards the utility's data center. The method has been elaborated on a real world case study. By applying the method to a real world topology, a source of error arise from the modeling process in which service cable was neglected. This issue has been elaborated through an example and a solution was presented in the form of an empirical threshold value.

ACKNOWLEDGEMENTS

Project no. 131501 has been implemented with the support provided from the National Research, Development and Innovation Fund of Hungary, financed under the K_19 funding scheme. A. Magyar was supported by the János Bolyai Research Scholarship of the Hungarian Academy of Sciences. Attila Magyar was supported by the ÚNKP-21-5 New National Excellence Program of the Ministry for Innovation and Technology from the source of the National Research, Development and Innovation Fund.

REFERENCES

Aucoin, B.M. and Russell, B.D. (1982). Distribution high impedance fault detection utilizing high frequency

current components. *IEEE Power Engineering Review*, PER-2(6), 46–47. doi:10.1109/MPER.1982.5521003.

Bula, I., Hoxha, V., Shala, M., and Hajrizi, E. (2016). Minimizing non-technical losses with point-to-point measurement of voltage drop between "smart" meters. *IFAC-PapersOnLine*, 49(29), 206 – 211. doi:https://doi.org/10.1016/j.ifacol.2016.11.103. 17th IFAC Conference on International Stability, Technology and Culture TECIS 2016.

Chakraborty, S. and Das, S. (2019). Application of smart meters in high impedance fault detection on distribution systems. *IEEE Transactions on Smart Grid*, 10(3), 3465–3473. doi:10.1109/TSG.2018.2828414.

Greber, M., Fodor, A., and Magyar, A. (2020). Generalized persistent fault detection in distribution systems using network flow theory. *IFAC-PapersOnLine*, 53(2), 13568–13574. doi:https://doi.org/10.1016/j.ifacol.2020.12.802. 21st IFAC World Congress.

Jota, F.G. and Jota, P.R.S. (1998). High-impedance fault identification using a fuzzy reasoning system. *IEE Proceedings - Generation, Transmission and Distribution*, 145(6), 656–661. doi:10.1049/ip-gtd:19982358.

Kodaira, D. and Han, S. (2018). Topology-based estimation of missing smart meter readings. *Energies*, 11(1), 224. doi:10.3390/en11010224. URL `https://doi.org/10.3390/en11010224`.

Le, T.N., Chin, W.L., Truong, D.K., and Nguyen, T.H. (2016). Advanced metering infrastructure based on smart meters in smart grid. In *Smart Metering Technology and Services - Inspirations for Energy Utilities*. InTech. doi:10.5772/63631. URL `https://doi.org/10.5772/63631`.

Ornelas, G.C., da Silva, M.V., Milanezi, J., da Costa, J.P.C., Maranhão, J.P.A., de Deus, F.E., and Galdo, G.D. (2016). First step towards a smart grid communication architecture for the brazilian federal district. *IFAC-PapersOnLine*, 49(30), 251 – 256. doi:https://doi.org/10.1016/j.ifacol.2016.11.120. 4th IFAC Symposium on Telematics Applications TA 2016.

Penshanwar, M.K., Gavande, M., and Satarkar, M.F.A.R. (2015). Phasor measurement unit technology and its applications - a review. In *2015 International Conference on Energy Systems and Applications*, 318–323. doi:10.1109/ICESA.2015.7503363.

Prakash, P. (2018). Data concentrators: The core of energy and data management,. Technical report, Texas Instruments.

Rusitschka, S., Eger, K., and Gerdes, C. (2010). Smart grid data cloud: A model for utilizing cloud computing in the smart grid domain. In *2010 First IEEE International Conference on Smart Grid Communications*, 483–488. doi:10.1109/SMARTGRID.2010.5622089.

Takagi, T., Yamakoshi, Y., Yamaura, M., Kondow, R., and Matsushima, T. (1982). Development of a new type fault locator using the one-terminal voltage and current data. *IEEE Transactions on Power Apparatus and Systems*, PAS-101(8), 2892–2898. doi:10.1109/TPAS.1982.317615.